SIMULATION OF HIGH-POWER TUNABLE THz GENERATION IN CORRUGATED PLASMA WAVEGUIDES*

Chenlong Miao†, IREAP, University of Maryland, College Park 20740, USA
John P. Palastro, Naval Research Laboratory, Washington DC 20375, USA
Thomas M. Antonsen, IREAP, University of Maryland, College Park 20740, USA

Abstract

Intense, short laser pulses propagating through inhomogeneous plasmas generate terahertz (THz) radiation. We consider the excitation of THz radiation by the interaction between an ultra short laser pulse and a miniature plasma waveguide. Such corrugated plasma waveguides support electromagnetic (EM) channel modes with subluminal phase velocities, thus allowing the phasing matching between the generated THz modes and the ponderomotive potential associated with laser pulse, making significant THz generation possible. Full format PIC simulations and theoretical analysis are conducted to investigate this slow wave phase matching mechanism. We find the generated THz is characterized by lateral emission from the channel, with a spectrum that may be narrow or broad depending on laser intensities. A range of realistic laser pulses and plasma profile parameters are considered with the goal of maximizing the conversion efficiency of optical energy to THz radiation. These studies are the first to investigate ponderomotively driven THz self-consistently in the interesting situations in which the interaction occurs over a scale many wavelengths long.

INTRODUCTION

Terahertz radiation (THz) lies between microwave and infrared in the electromagnetic spectrum and typically spans frequencies from 300 GHz to 20 THz. A wide variety of applications [1] can be found including time domain spectroscopy (TDS), remote detection, medical and biological imaging and so on. One of the most commonly seen examples is that most airports use millimeter wave/THz scanners for human body security checking. Existing small scale THz sources based on laser-solid interaction are limited to μJ/pulse levels due to material damage [2] although the recent discovery using optical rectification (OR) [3–5] in organic crystals can exceed this limit. This has led to the consideration of THz generation via laser-plasma interactions [6–8] and THz peak energy of tens of μJ can be achieved. Higher energy THz pulses can be generated at accelerator facilities via synchrotron [9] or transition radiation [10]. Such facilities are relatively large and expensive to operate. This motivates research interest in small-scale, high efficiency terahertz sources.

A scheme involving laser pulses propagating through axially corrugated plasma channels has been proposed by Antonsen et at. [11]. This slow wave structure supports electromagnetic modes that have subluminal phase velocities, thus providing the possibility of phase matching between the excited modes and the driver. Here, with a combination of theory and simulaition, we investigated the ponderomotively driven THz generation via the slow wave phase matching process by laser pulses propagating through corrugated plasma waveguides. These waveguides have been realized in laboratory [12, 13].

THz GENERATION

The set up of of the THz generation mechanism is schematically shown in Fig. 1.

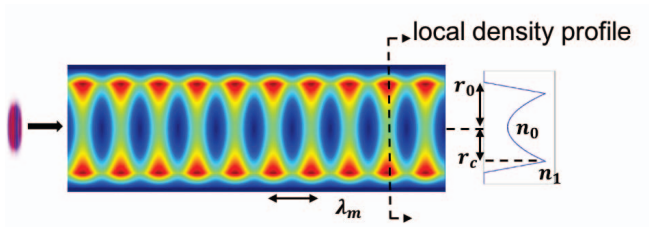

Figure 1: System setup of THz generation in corrugated plasma waveguides. An intense, ultra-short laser pulse propagates through the preformed corrugated plasma channels and drives lateral THz emission.

Corrugated Plasma Waveguides

We consider the corrugated plasma waveguides as shown in Fig. 1 to be cylindrical symmetric, with electron densities described by the following,

$$\frac{n(r,z)}{n_{00}} = \begin{cases} n_0 + (n_1 - n_0)\dfrac{r^2}{r_c^2} & r \le r_c \\ n_1 \dfrac{r_0 - r}{r_0 - r_c} & r_c < r < r_0 \\ 0 & r \ge r_0 \end{cases} \quad (1)$$

where n_{00} is the normalized density. The channel has a density modulation period of λ_m and the modulation wavenumber is defined as $k_m = 2\pi/\lambda_m$. The axially modulated z dependence is carried through the parameters n_0, n_1, r_c and r_0. The quantity $n_0(z)$ is the normalized on-axis density and $n_1(z)$ is normalized density at $r = r_c$ as shown in Fig. 1. The quantities n_0 and n_1 are both axially modulated, $n_0 = 1+\delta \sin(k_m z)$ and $n_1 = \overline{n}_1+\delta_1 \sin(k_m z)$, respectively. δ is the density modulation amplitude of on-axis density n_0. The quantity $\overline{n}_1$ is the average transverse peak density and δ_1 is the density modulation amplitude of n_1. The density

* Work supported by DoE and NRL
† clmiao@umd.edu

has a parabolic transverse profile to guide the laser pulse during propagation. The quantity r_c is the radius at which n_1 characterizes the density, and the density then decreases linearly to zero between r_c and r_0. The quantities r_c and r_0 may also be axially modulated.

Simulation Setup and THz Mode Excitation

THz generation in corrugated plasma waveguides is simulated using the full format PIC code TurboWAVE [14]. The simulations, performed in 2D planar geometry, employ a finite sized plasma channel illuminated by a laser pulse incident from the interface. Fig. 2 shows a false color image of the transverse component of Poynting flux P_x after the laser pulse traverses the channel. The plasma wave excitation can be observed as the rapid oscillations inside the channel and the alternate positive and negative values of the Poynting flux indicate a small average flux. However, at both lateral boundaries, one can observe the THz emission as the red and blue streaks denoting the lateral Poynting flux.

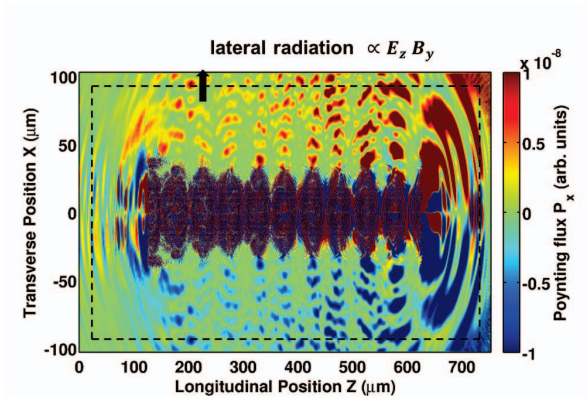

Figure 2: Simulation setup. The Poynting flux through each surface is calculated to diagnose radiated THz energy.

The radiated spectral density for the case of $a_0 = 0.4$, where a_0 is the normalized laser vector potential, is displayed in Fig. 3. The plasma channel consists of 10 modulation periods with the following parameters: $\lambda_m = 50\ \mu m$, $n_{00} = 1.4 \times 10^{18}\ cm^{-3}$, $\delta_1 = \delta = 0.9$, $\overline{n}_1 = 3$, $r_c = 30\ \mu m$ and $r_0 = 40\ \mu m$. We can observe an appreciable amount of lateral radiation is generated as the fundamental mode dominates, followed by the excitation of higher order modes, while in the case of an axially uniform plasma, there is no measurable lateral THz emission except for the resonant transition radiation [15–17] generated as the laser pulse crosses the vacuum plasma interface.

THz Dependence on Plasma Density

Shown in Fig. 4 is the radiated THz spectral density for different plasma densities in the case of $a_0 = 0.4$. As the plasma density varies, the radiation peaks change and the central frequencies of these peaks follow the fundamental mode of the channel. As the plasma density varies form $1.4 \times 10^{18}\ cm^{-3}$ to $0.07 \times 10^{18}\ cm^{-3}$, the frequency of the

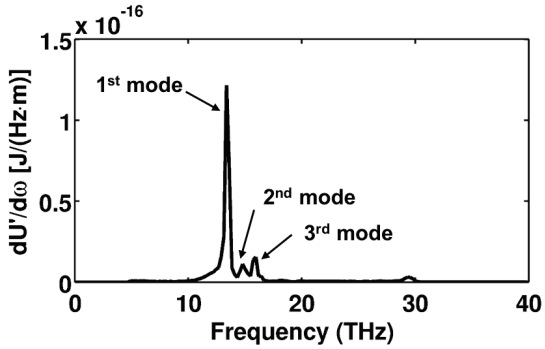

Figure 3: Radiated THz spectrum shows different THz modes are excited. The frequency of each excited mode matches well with the phase matching condition we obtained.

fundamental mode decreases, and most importantly, the ratio of the generation of electromagnetic radiation at these frequencies over plasma waves increases. In particular, more energy extracted from the driver pulse is converted into THz radiation due to the fact that the central channel density is tending low and the excitation of plasma waves becomes small. As a result, at an averaged on axis density around $1.75 \times 10^{17}\ cm^{-3}$, the THz generation peaks at the fundamental frequency of 6.6 THz corresponding to the local maxima of coupling. At the same time, more THz radiation escapes channel since the radial density barrier is lower compared with higher plasma density.

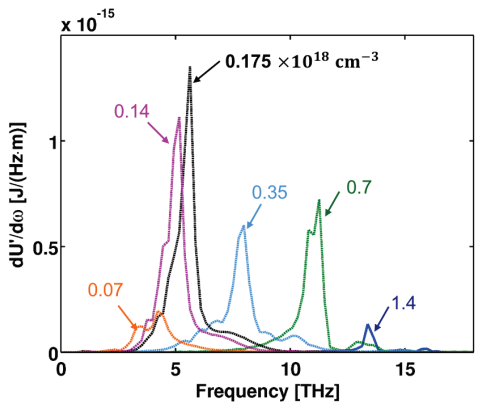

Figure 4: Radiated THz spectral density $dU'/d\omega$ for different plasma densities.

THz Dependence on Laser Intensity

Ponderomotively driven THz radiation is expected to scale quadratically as the laser intensity, i.e., $E_{THz} \sim a_0^4/\gamma^2 \sim a_0^4/(1 + a_0^2)$. It is expected the generated THz energy can be enhanced by increasing laser intensities. In the linear regime ($a_0 << 1$), the ponderomotive driven THz radiation scales as a_0^4, one may think the scaling should be weaker in the for high laser intensities ($a_0 > 1$) due to the increase of effective electron mass resulting from quiver velocity. However, as shown in Fig. 5, for larger a_0, the radiated THz energy E_{THz} is enhanced above the scaling estimate. This

enhancement phenomenon is accompanied by a change in the spectrum. It is shown in this case higher order channel modes are excited by nonlinear currents and interference between higher order modes is also observed. Our goal is to optimize the efficiency of the optical laser pulse energy converted to THz, we define a relative conversion efficiency as the ratio of the generated THz energy over the depleted laser energy, $\eta = E_{THz}/|\Delta E_{Laser}|$. By maximizing this efficiency, less laser power is expended in plasma wave, thus freeing it to drive THz for longer distances. As displayed in Fig. 5, for $a_0 << 1$, it follows the linear theory, while for $a_0 > 1$, higher scaling is observed.

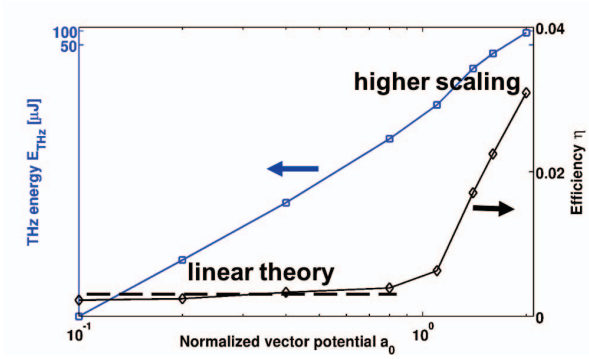

Figure 5: Radiated THz energy E_{THz} (blue) and relative conversion efficiency (black) for different a_0.

THz Scaling with Plasma Channel Length

Our study is the first to study the THz generation in the nonlinear regime including generation of nonlinear plasma wakes and Self consistent evolution of the driving laser pulse. Simulation result displayed in Fig. 6 shows that around 80% of the energy stored in the laser pulse is depleted within the propagation distance of 1.5 cm. It is also shown that the rate dU'/dZ of THz energy generation increases with distance as the normalized vector potential increases during propagation due to the action conservation. As a result, within the same propagation distance, THz energy of 37.8 mJ is generated, more than 8% of the depleted pulse energy is converted into THz radiation.

Different Channel Structrures

Shown in Fig. 7 is another experimentally demonstrated channel type with on axis density peaks. For $a_0 = 0.4$, enhancement of fundamental THz modes is observed and can be explained by the excitation of a higher electron current since the driver pulse encounters more electrons on-axis at the local density maximum for the density profile. In addition, the axially averaged density profile has a lower density barrier that allows the generated THz waves to better escape the channel. For the higher laser intensity case, the generated THz is characterized by a different spectrum compared with the previous structure with off-axis density peaks. Although the amount of THz energy is enhanced for both cases, the spectrum is still confined in a relatively

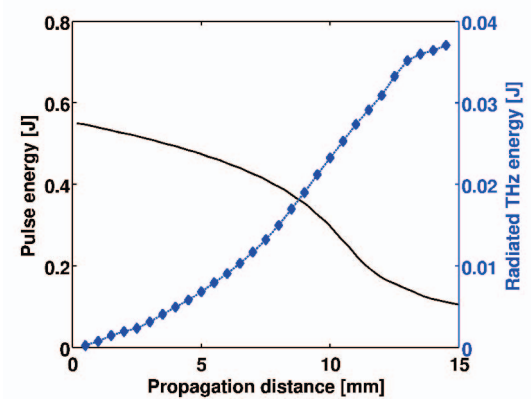

Figure 6: Pulse energy depletion (black, solid) of an initial laser with $a_0 = 2.0$ (0.55 J) during the propagation in a corrugated plasma channel. Scaling of Radiated THz energy (blue, dashed) versus propagation distance shows the generated THz energy is higher than the linear scaling with distance.

narrow band fundamental frequency, while in the previous case higher order THz modes are significantly generated and consequently modify the spectrum.

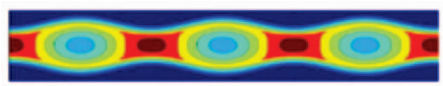

Figure 7: A new channel structure with on-axis density peaks.

CONCLUSION

Ponderomotively driven currents can be phase matched to the subluminal EM modes supported by the axially corrugated plasma waveguides, thus generating THz radiation. Different approaches are investigated to maximize the efficiency of the optical laser pulse energy converted to THz. We find THz spectrum is easily tunable by modifying channel parameters. As an example, a fixed driver pulse (0.55 J) with spot size of 15 μm and pulse duration of 15 fs excites approximately 37.8 mJ of THz radiation in a 1.5 cm corrugated plasma waveguide with on axis average density of $1.4 \times 10^{18}\ cm^{-3}$.

ACKNOWLEDGEMENT

The authors would like to acknowledge Dr. Daniel Gordon for the use of TurboWAVE. Part of the simulations was performed on NERSC Edison and Deepthought2 clusters at UMD.

REFERENCES

[1] M. Sherwin, C. Schmuttenmaer, and P. Bucksbaum, in *Report of a DOE-NSF-NIHWorkshop, Arlington, VA, 2004 (unpublished)*, Vol. 12 (2004) p. 14.

[2] E. Budiarto, J. Margolies, S. Jeong, J. Son, and J. Bokor, *IEEE J. Sel. Top. Quantum Electron.* 32, 1839 (1996).

[3] C. Vicario, A. V. Ovchinnikov, S. I. Ashitkov, M. B. Agranat, V. E. Fortov, and C. P. Hauri, *Opt. Lett*. 39, 6632 (2014).

[4] X. Wu, C. Zhou, W. R. Huang, F. Ahr, and F. X. Kärtner, *Opt. Express* 23, 29729 (2015).

[5] J. A. Fülöp, Z. Ollmann, *et al.*, *Opt. Express* 22, 20155 (2014).

[6] W. P. Leemans, C. G. R. Geddes, *et al.*, *Phys. Rev. Lett.* 91, 074802 (2003).

[7] K.-Y. Kim, A. Taylor, J. Glownia, and G. Rodriguez, *Nat. Photonics* 2, 605 (2008).

[8] A. Gopal, S. Herzer, *et al.*, *Phys. Rev. Lett.* 111, 074802 (2013).

[9] T. Nakazato, M. Oyamada, *et al.*, *Phys. Rev. Lett.* 63, 1245 (1989).

[10] U. Happek, A. J. Sievers, and E. B. Blum, *Phys. Rev. Lett.* 67, 2962 (1991).

[11] T. M. Antonsen, J. P. Palastro, and H. M. Milchberg, *Phys. Plasmas* 14, 033107 (2007).

[12] B. D. Layer, A. York, et al., Phys. Rev. Lett. 99, 035001 (2007).

[13] G. A. Hine, A. J. Goers, L. Feder, J. A. Elle, S. J. Yoon, and H. M. Milchberg, *Opt. Lett.* 41, 3427 (2016).

[14] D. F. Gordon, IEEE Trans. Plasma Sci. 35, 1486 (2007).

[15] C. Miao, J. P. Palastro, and T. M. Antonsen, *Phys. Plasmas* 23, 063103 (2016).

[16] C. Miao, J. P. Palastro, and T. M. Antonsen, in *6th International Particle Accelerator Conference (IPAC 15) (2015)* p. 2661, paper WEPWA068.

[17] C. Miao, J. P. Palastro, A. J. Pearson, and T. M. Antonsen, in *2015 40th International Conference on Infrared, Millimeter, and Terahertz waves (IRMMW-THz)* (2015) pp. 1-2.